Published in final edited form as:
Alcohol Clin Exp Res. 2013 May ; 37(5): 748–756. doi:10.1111/acer.12024.

Global functional connectivity abnormalities in children with Fetal Alcohol Spectrum Disorders (FASD)

Jeffrey R. Wozniak, **Bryon A. Mueller**, **Christopher J. Bell**, **Ryan L. Muetzel**, **Heather L. Hoecker**, **Christopher J. Boys**, and **Kelvin O. Lim**
University of Minnesota - Twin Cities

Abstract

Background—Previous studies, including those employing Diffusion Tensor Imaging (DTI), have revealed significant disturbances in the white matter of individuals with Fetal Alcohol Spectrum Disorders (FASD). Both macrostructural and microstructural abnormalities have been observed across levels of FASD severity. Emerging evidence suggests that these white matter abnormalities are associated with functional deficits. This study used resting-state fMRI to evaluate the status of network functional connectivity in children with FASD compared to control subjects.

Methods—Participants included 24 children with FASD, ages 10–17, and 31 matched controls. Neurocognitive tests were administered including Wechsler Intelligence Scales, California Verbal Learning Test, and Behavior Rating Inventory of Executive Functioning. High resolution anatomical MRI data and six-minute resting-state fMRI data were collected. The resting-state fMRI data were subjected to a graph theory analysis and four global measures of cortical network connectivity were computed: characteristic path length, mean clustering coefficient, local efficiency, and global efficiency.

Results—Results revealed significantly altered network connectivity in those with FASD. The characteristic path length was 3.1% higher (p=.04, Cohen's d=.47) and global efficiency was 1.9% lower (p=.04, d=.63) in children with FASD compared to controls, suggesting decreased network capacity that may have implications for integrative cognitive functioning. Global efficiency was significantly positively correlated with cortical thickness in frontal (r=.38, p=.005), temporal (r=.28, p=.043), and parietal (r=.36, p=.008) regions. No relationship between facial dysmorphology and functional connectivity was observed. Exploratory correlations suggested that global efficiency and characteristic path length are associated with capacity for immediate verbal memory on the CVLT (r=.41, p=.05 and r=.41, p=.01 respectively) among those with FASD.

Conclusions—Resting-state functional connectivity measures provide new insight into the integrity of brain networks in clinical populations such as FASD. Results demonstrate that children with FASD have alterations in core components of network function and that these aspects of brain integrity are related to measures of structure and cognitive functioning.

Keywords

Fetal alcohol (FAS, FASD); Brain; functional MRI (fMRI); resting-state; connectivity; neuropsychological

Correspondence: Jeffrey R. Wozniak, Ph.D., Department of Psychiatry, University of Minnesota, F256/2B West, 2450 Riverside Ave., Minneapolis, MN, 55454, 612-273-9741, 612-273-9779 (FAX), jwozniak@umn.edu.

INTRODUCTION

Although numerous brain anomalies are recognized in Fetal Alcohol Spectrum Disorders (FASD) (Riley et al., 2004), there is mounting evidence that white matter may be disproportionately impacted. In early studies, complete agenesis of the corpus callosum was reported and other callosal abnormalities were seen including thinning, hypoplasia, and partial agenesis (Riley et al., 1995). Volumetric MRI studies show that prenatal alcohol exposure is associated with widespread abnormalities in white matter macrostructure beyond the corpus callosum (Archibald et al., 2001). Diffusion Tensor Imaging (DTI) provides further evidence of white matter pathology in FASD including microstructural abnormalities in corpus callosum (Ma et al., 2005; Wozniak et al., 2006) – but also elsewhere in the brain (Fryer et al., 2009; Lebel et al., 2008; Sowell et al., 2008a; Spottiswoode et al., 2011). This disruption in white matter microstructure is associated with cognitive dysfunction in FASD including abnormal conditioned-response learning (Spottiswoode et al., 2011), visual-motor deficits (Sowell et al., 2008a) and poor perceptual organization (Wozniak et al., 2009).

Based on consistent findings of *structural* connectivity disturbances in FASD, we sought to understand the impact of these abnormalities on *functional* connectivity. We first conducted a DTI-tractography/fMRI study to evaluate inter-hemispheric functional connectivity in brain regions with underlying microstructural abnormalities in FASD, especially in posterior corpus callosum (Wozniak et al., 2011). Results demonstrated a disturbance in inter-hemispheric connectivity as evident by low right-left correlations in resting-fMRI signal for FASD compared to controls. This was especially evident for right and left para-central cortical regions, which are heavily inter-connected by posterior callosal projection fibers. The current study sought to extend our understanding of functional connectivity in FASD beyond individual regions toward an examination of global cortical connectivity. This study utilized global metrics that can be compared readily across groups and can be evaluated against other important clinical characteristics of FASD including cognitive functioning. We explicitly set out to examine global connectivity rather than individual functional network or specific region-to-region connectivity because: 1) the effects of alcohol on the developing brain have been shown to be so widespread rather than discrete; 2) there is value in characterizing the overall severity of brain effects of prenatal alcohol exposure; and 3) measures of global brain functioning will ultimately have great utility in FASD intervention studies.

“Functional connectivity” characterizes distributed brain activity that is coordinated in time and space across brain. Friston (1993) described it as the “temporal correlation between spatially remote neurophysical events”. Functional connectivity studies often measure brain activity during rest. Correlations in fMRI data can be used to “map” brain networks based on regionally synchronized activity (Biswal et al., 1995). Networks can be extracted empirically with independent components analysis (ICA) or seed-based strategies can be employed. As one example, Raichle et al. (2001) described a “default mode network” – a set of brain regions that operate as a “system” in real-time when the subject is disengaged from tasks. Resting-state networks are involved in non-task, off-line activities including memory consolidation and planning (Raichle and Snyder, 2007). These networks follow developmental trajectories; child “task” networks are characterized by high local connectivity and lower long-distance connectivity than adults (Fair et al., 2009). In task networks, local connectivity decreases with age and long-distance connectivity increases. In contrast, the default-mode network has relatively few local connections in children, but subsequently matures to a more distributed form by adulthood (Fair et al., 2008).

Previous studies have demonstrated that functional brain activity fits small world network parameters both temporally and spatially (Bassett and Bullmore, 2006). Small world

networks are characterized by highly clustered, modular processing centers – along with a few highly efficient long-distance communication paths (Rubinov and Sporns, 2010). In a small world network, individual nodes (brain regions in this case) are highly connected with neighboring regions (clustered) and long-distance communication is enhanced by a few "short-cuts" that facilitate efficient jumps between distant regions without traversing all intervening nodes (Watts and Strogatz, 1998). In the brain, white matter provides these highly efficient routes between distant grey matter regions where more modular/clustered processing occurs.

Graph theory provides a set of robust metrics for evaluating the properties of small-world networks (Achard and Bullmore, 2007). One standard metric, *mean clustering coefficient*, reflects the density of connections between neighbors surrounding a single node. High *clustering* is a defining characteristic of small-world networks. *Local efficiency* is the mean of the efficiency of local sub-graphs and is a measure of "connectedness" at the neighborhood level. Local efficiency reflects the "fault tolerance" of a network; it characterizes the remaining efficiency of local connections when a node is removed (Latora and Marchiori, 2001). A third metric, *characteristic path length*, is the length of the shortest connections between pairs of nodes (averaged over the brain) and is a measure of serial information transfer between nodes. Small-world networks are characterized by short path-length that yields efficient long-distance communication. Lastly, the mean of the inverse of path length, *global efficiency*, similarly reflects communication efficiency but accounts for parallel information transfer (which occurs on a massive scale in the brain). Global efficiency has the advantage of being robust even with networks that are not fully connected (Achard and Bullmore, 2007) and is particularly useful in evaluating pathological networks. Overall, small-world network topology reflects a balance between network *segregation* (local clusters) and *integration* (efficient communication between clusters) (Sporns and Zwi, 2004). The clinical relevance of connectivity measures is illustrated by studies showing relationships between network characteristics like path length and IQ (networks with greater path length are less efficient and are associated with lower IQ) (van den Heuvel et al., 2009).

To date, there are very few functional MRI studies of FASD and only two previous studies that examined resting-state functional connectivity (Santhanam et al., 2011; Wozniak et al., 2011). The Santhanam study examined the default mode network comprising medial prefrontal cortex, posterior cingulate, precuneus, inferior parietal, and medial temporal regions; it shows increased activity during non-task periods. The expected network "deactivation" upon initiation of an arithmetic task was abnormal in prenatally-exposed adults with dysmorphic facial features. The findings suggest that resting-state networks normally work in conjunction with "active" cognitive networks – each inhibiting the other in turn – and that dysfunction may occur at the level of coordinating these alternating networks. Task-based fMRI studies have also revealed functional connectivity abnormalities in FASD, including alterations in frontostriatal coupling (Roussotte et al., 2012).

Based on what is known about the widespread effects of prenatal alcohol exposure on both grey and white matter development, we hypothesized that global cortical functional connectivity would be disturbed in children with FASD. We expected to see low network efficiency and evidence of disconnectivity. Summary measures of network connectivity were expected to correlate with cognitive functioning including components of IQ, memory, and executive functioning. In all cases, we expected to see low network efficiency and poor overall connectivity to be associated with greater cognitive impairment.

MATERIALS AND METHODS

Participants

Participants, ages 10–17, were all right-handed. Thirty-two children with FASD were recruited from the University of Minnesota's FASD Clinic. Thirty-three control subjects with no prenatal alcohol exposure were recruited from the Twin Cities metropolitan area from diverse neighborhoods and socioeconomic levels. Participants with FASD were seen by a pediatric psychologist and developmental pediatrician with formal training and more than twelve years experience using the 4-Digit Diagnostic System (Astley and Clarren, 2000). Participants with FASD were assessed for alcohol and other drug use as part of their clinical work-up and again as part of a telephone screening with the parent.

The 4-Digit Diagnostic system classifies individuals on: 1) growth, 2) facial characteristics, 3) Central Nervous System (CNS), and 4) alcohol exposure (Astley and Clarren, 2000). FAS is defined by growth deficiency (<10^{th} percentile height and weight or <3^{rd} percentile on either), severe facial abnormalities (thin upper lip, smooth philtrum, and palpebral fissure width more than 2 SD below the mean), moderate or severe CNS impairment (microcephaly and/or cognitive deficits more than 2 SD below the mean in three domains), and confirmed prenatal alcohol exposure. Partial FAS (pFAS) is characterized by at least moderate facial abnormalities (one or more of: thin upper lip, smooth philtrum, or palpebral fissure width more than 2 SD below the mean), moderate or severe CNS impairment, and confirmed prenatal alcohol exposure. Static Encephalopathy is characterized by moderate or severe CNS impairment. For pFAS, confirmed maternal alcohol consumption is required at either a "high risk" level (estimated >100 mg/dl blood alcohol concentration weekly, early in pregnancy) or a lower level that is associated with "some risk." For Static Encephalopathy, maternal alcohol exposure may be either confirmed as heavy or may be only suspected - but only when facial dysmorphology is also present. For maximum clarity to all readers, we have also classified all FASD participants in Table 1 according to the modified Institute of Medicine criteria (Hoyme et al., 2005).

Eight participants with FASD were excluded for excessive motion during MRI; one control subject was excluded for motion and one additional control subject did not meet the threshold for a fully-connected network (see below). These exclusions resulted in 24 FASD participants and 31 controls with good fMRI data. Table 1 contains the participant demographics.

Of the 24 participants with FASD, 20 had confirmed documentation of prenatal alcohol exposure (self-report by the biological parent or social service records indicating heavy maternal use during pregnancy). Four FASD participants had only suspected exposure, but each had FASD facial characteristics and cognitive deficits. Participants were excluded if alcohol exposure was minimal (e.g. a single drink on occasion). FASD participants were excluded for other documented heavy prenatal drug exposure (except nicotine and caffeine), although there was suspicion of maternal cocaine use in two cases and suspicion of marijuana use in four cases, but the extent of use was unknown. In all cases, alcohol was the predominant substance of abuse.

Additional exclusion criteria for all subjects were developmental disorder (ex. Autism), very low birthweight (<1500 grams), neurological disorder, traumatic brain injury, medical condition affecting the brain, substance use by the participant, or contraindications to safe MRI scanning. Control subjects were excluded for parent-reported history of prenatal substance exposure, substance use (including alcohol use) by the participant (assessed during a telephone screening with the parent), and for psychiatric disorder or learning disability. Psychiatric co-morbidity (see Table 1) was not an exclusion criterion for

participants with FASD because it is well-recognized that co-morbidity is high in FASD (Streissguth and O'Malley, 2000). Participants' medications (see Table 1) were not altered for this study.

Participants underwent a University of Minnesota IRB-approved consent process and were compensated for their time.

Neuropsychological Evaluation

Participants were administered either the Wechsler Intelligence Scales for Children – Fourth Edition (WISC-IV) (Wechsler, 2003) (ages 10–16) or the Wechsler Adult Intelligence Scales – Third Edition (WAIS-III) (Wechsler, 1997) (age 17) and either the California Verbal Learning Test – Children's Version (CVLT-C) (Delis et al., 1994) or the Adult Version (CVLT-II) (Delis et al., 2000) by a psychometrist. Parents competed the Behavior Rating Inventory of Executive Functioning (BRIEF) (Gioia et al., 2000).

MRI acquisition procedures

Subjects were scanned on a Siemens 3T TIM Trio MRI scanner with a 12-channel parallel array head coil. The imaging sequence included a structural T1-weighted scan, a resting-state fMRI scan, and a field map scan; details of the specific parameters are in Table 2. During the resting-state scan, participants were instructed to close their eyes and remain still. MRI scans were performed within one year of the neurocognitive tests. Participants were not sedated for the MRI scan nor were their usual medications modified.

MRI processing

Resting-state fMRI processing—The fMRI data were processed using a slightly modified version of the 1000 Functional Connectome (TFC) pre-processing scripts (www.nitrc.org/plugins/mwiki/index.php/fcon_1000). Tools from AFNI (Cox, 1996) and the FMRIB Software Library (FSL) version 4.1.6 (Smith et al., 2004; Woolrich et al., 2009) were used in the TFC processing. This included skull stripping, motion correction, geometric distortion correction using FSL's FUGUE (added to the TFC pipeline), spatial smoothing (FWHM of 6 mm), grand mean scaling, band pass temporal filtering (0.005 to 0.1 Hz), and quadratic de-trending. The TFC processing of the T1 volume included skull stripping and FSL's FAST tissue segmentation to define whole brain, white matter and ventricular cerebrospinal fluid (CSF) regions of interest (ROIs). The skull-stripped T1 and tissue segmentation ROIs were registered to the fMRI data using FSL's FLIRT. Timecourses from the three tissue segmentation ROIs, along with the six motion parameters, were used as voxel-wise nuisance regressors in the TFC processing of the fMRI data.

T1 cortical parcellation—Cortical parcellation of the T1 volume was done with FreeSurfer version 4.5 (surfer.nmr.mgh.harvard.edu) (Dale et al., 1999). Processing included removal of non-brain tissue, automated Talairach transformation, segmentation, intensity normalization, tessellation of the grey matter/white matter boundary, topology correction, surface deformation, and automated parcellation of the cortical grey matter into 34 ROIs per hemisphere. Each subject's data was visually inspected by a trained operator (C.J.B.) to ensure accuracy of the cortical parcellation. Hand editing was not employed.

Time-series extraction—The 68 Freesurfer cortical parcellations (34 per hemisphere) were registered to the TFC-processed fMRI data using Freesurfer's bbregister (Greve and Fischl, 2009). The parcellations were dilated during registration but none were allowed to overlap and voxels outside the TFC brain-mask were excluded. ROIs that contained fewer than 10 fMRI voxels for any subject were excluded from the final analysis. This resulted in the exclusion of 6 ROIs (bilateral entorhinal, frontal pole and temporal pole), leaving a total

of 62 ROIs (31 per hemisphere). The mean fMRI time-series of all voxels within each ROI were then extracted for each subject.

Computation of the network metrics—Pearson correlations were computed between the time-series from all possible pairs of the 62 cortical ROIs using MATLAB (Mathworks, Natick, MA). Graph theory network metrics were computed for each subject's Pearson correlation matrix (Bullmore and Sporns, 2009; Rubinov and Sporns, 2010) utilizing tools from the BCT toolbox (http://sites.google.com/a/brain-connectivity-toolbox.net/bct/Home). Cortical ROIs served as network nodes and correlation values served as the connections (edges). The cost of a network is defined as the ratio of existing connections to the total number of possible connections in the graph ((62*61)/2 = 1891 for a 62 node network). Binary, non-directional adjacency matrices were determined by applying a subject-specific threshold to each subject's data across a range of costs from 0.1 to 0.5, with 0.05 step increments. Four metrics of interest were *characteristic path length*, *mean clustering coefficient*, *local efficiency* and *global efficiency* (Latora and Marchiori, 2001; Watts and Strogatz, 1998).

Path length is the smallest number of connections that must be traversed to connect any pair of nodes in the network. The *characteristic path length* is the average *path length* between all pairs of nodes in the network. A higher than normal characteristic path length implies less reliance on highly efficient hubs for long distance communication and more reliance on multiple smaller "jumps" between regions. The *mean clustering coefficient* reflects the density of local connections. *Global efficiency*, inversely related to path length, reflects properties of the network associated with long-range connections that facilitate rapid communication between remote brain regions; it reflects the network's capacity for parallel information propagation. In contrast, *local efficiency* reflects properties of the network associated with modular processing within more localized brain regions (Latora and Marchiori, 2001).

In network graph mathematics, cost has implications for overall topology of the network and there are multiple costs at which the network metrics can be examined. We examined the network at the minimum cost at which all participants had fully-connected networks. A fully-connected network contains at least one possible pathway between every node. All participants except one control subject had fully-connected networks at a cost of 0.20 (at which 20% of all possible node-to-node connections are made). At costs above 0.20, many subject's networks lost small world properties (sigma < 1.5) (Bassett and Bullmore, 2006).

RESULTS

Testing for group differences in motion—Motion during fMRI can lead to spurious correlations in voxel intensity, even after the TFC processing stream (motion correction followed by regression against the six motion timecourses and CSF, WM and whole brain timecourses). Translational and angular motion were examined (Liu et al., 2008). Included participants had less than 1.3 mm of translational displacement and less than 0.015 radians of angular displacement (maximum volume to volume displacements). The root mean square (RMS) of translational and angular movements (similar to the averaged amount of movement across all fMRI volumes) was less than 0.17 mm. (translational displacement) and 0.0015 radians (angular displacement) for included subjects. These thresholds resulted in the exclusion of one control and eight FASD participants. A group comparison tested for differences in RMS motion for the remaining participants. Independent samples t-tests revealed no group difference in the amount of translation [t (1,52)=1.27, p=.209] or rotation [t(1,52)=.391, p=.697]. Therefore, motion was not entered as a covariate in any of the remaining analyses.

Examining group differences in network connectivity—There was not a group difference in minimum cost to achieve a fully-connected network, [t(1,53)=−.214, p=.831]. Mean costs to fully-connect were 0.121 (±0.03) for the control group and 0.123 (±0.03) for the FASD group. There was no group difference in threshold to achieve a cost of 0.20, [t(1,53)= −1.30, p=.897. Mean threshold to obtain a cost of 0.20 was 0.263 (±0.24) for the control group and 0.264 (±0.04) for the FASD group. Across costs, there was not a group difference in small-world index or sigma, [t(1,53)=.609, p=.545]. At the cost examined (0.20), sigma was 2.17 (±0.19) for controls and 2.13 (±0.21) for FASD. Thus, the graph theory metrics in the following analyses were computed for networks with equivalent parameters.

Table 3 contains means and effect sizes for global cortical network connectivity measures with adjacency matrices evaluated at a cost of 0.20. There was a significant group difference in *characteristic path length*, [t(1,53)= −2.13, p=.038] with the FASD group having 3.1% higher path length compared to controls. The *mean clustering coefficient* differed at a trend level [t(1,53)= −1.87, p=.066] with the FASD group having 3.5% higher *mean clustering coefficient* compared to controls. There was a trend-level difference in *local efficiency* [t(1,53)= −1.70, p=.096], with the FASD group showing 1.3% higher local efficiency than controls. A significant group difference was observed for *global efficiency* [t(1,53)=2.08, p=.042], with the FASD group having 1.9% lower global efficiency than controls. Effect sizes for global efficiency, characteristic path length, and mean clustering coefficient were all in the medium range (Cohen, 1992).

There was no difference in *characteristic path length* for FASD participants taking any medication (n=14) vs. those taking no medications (n=10), [t(1,22)= −.14, p=.894] nor was there a difference for those taking stimulant medications (n=10) vs. those taking no medications (n=10), [t(1,22)= −.28, p=.782]. Similarly, there was no difference in *global efficiency* for FASD participants taking any medication vs. those taking no medications, [t(1,22)=.09, p=.932] nor was there a difference for those taking stimulant medications vs. those taking no medications [t(1,22)=.13, p=.897].

There was no difference in *characteristic path length* for FASD participants with co-morbid ADHD (n=15) vs. those without ADHD (n=9), [t(1,22)=.77, p=.449] nor was there a difference in *global efficiency* for participants with ADHD vs. those without ADHD, [t(1,22)= −.71, p=.4840.

Network connectivity and structural brain relationships—Regional brain volumes and cortical thicknesses measures were computed with FreeSurfer. Relationships between the two network connectivity measures that showed group differences (*characteristic path length* and *global efficiency*) and three volumetric measures were tested with Pearson correlations for the FASD group. Neither of the network measures was significantly correlated with cerebral cortex volume, white matter volume, or corpus callosum volume (all adjusted for whole-brain volume).

Previous studies have demonstrated both greater and lesser cortical thickness in FASD (Sowell et al., 2008b; Yang et al., 2011; Zhou et al., 2011), especially in frontal, temporal and parietal regions. In this study, cortical lobe thicknesses were computed by averaging across appropriate bilateral Freesurfer ROI cortical thickness measures, resulting in measures of *frontal*, *temporal*, *parietal*, and *occipital* thickness. There was not a significant group difference in mean frontal cortex thickness, [t(1,52)=.679, p=.500], temporal cortex thickness, [t(1,52)=.475, p=.667], parietal cortex thickness, [t(1,52)=.809, p=.422], or occipital cortex thickness [t(1,52)= −.484, p=.631]. Relationships between characteristic path length and global efficiency and these regional cortical thickness measures were

examined with Pearson correlations. Because there were no group differences in cortical thickness, these correlations were done across all subjects (FASD and controls combined). Table 4 contains the results.

In frontal, parietal, and temporal regions, cortical thickness was inversely correlated with characteristic path length (thinner cortex was associated with greater path length) and positively correlated with global efficiency (thicker cortex was associated with higher global efficiency). No association was seen for thickness in the occipital region. Figure 1 illustrates the relationship between frontal cortical thickness and global efficiency as an example. Because cortical thickness and network connectivity change over the age range we evaluated, a second set of correlations, with age partialled out, were conducted (see Table 4). The relationship between frontal lobe thickness and global efficiency remained significant, while the other correlations were reduced to a trend or non-significant level.

Network connectivity and physical manifestations of FASD—The relationship between global cortical connectivity and facial dysmorphology was examined in the FASD group with four ANOVAS, each testing for mean differences by facial rating (Astley& Clarren rank 1–4) for one of the four network metrics (characteristic path length, mean clustering coefficient, local efficiency, and global efficiency). None of these statistical tests was significant or at the trend level. Thus, network connectivity did not vary by level of facial abnormality.

Network connectivity and cognitive functioning—Exploratory tests examining the relationship between the network connectivity measures and cognitive performance were also conducted. Only the two network connectivity measures that showed group differences (*characteristic path length* and *global efficiency*) were examined. Results are in Table 5. Because there were group differences in cognitive performance, these correlations were only computed for participants with FASD.

Although none of these correlations survived Bonferroni correction, the strongest associations were seen with the immediate memory measure from the CVLT in contrast to the long-delay memory measure. Also noteworthy was the relatively strong association between characteristic path length and problems with executive functioning as noted by the BRIEF parent-report instrument. In this set of analyses, the network connectivity measures did not show any significant associations with measures of general intellectual functioning.

DISCUSSION

The findings complement our previous study that examined regional functional connectivity in children with FASD (Wozniak et al., 2011) and found inter-hemispheric connectivity abnormalities, notably in para-central cortical regions that are connected by posterior callosal fibers. MRI studies have consistently revealed posterior callosal macrostructural and microstructural anomalies in children with FASD (Bookstein et al., 2007; Fryer et al., 2009; Lebel et al., 2008; Li et al., 2009; Sowell et al., 2008a; Wozniak et al., 2006; Wozniak et al., 2009). Our findings suggest that those structural abnormalities have functional consequences at a very basic level.

We sought to extend our earlier findings to an evaluation of global cortical network connectivity. Brain structure and function are organized in terms of *small-world network* properties. Chief among these properties are high regional clustering of information processing combined with an efficient hub organization that facilitates long-distance communication. Small-world network organization maximizes communication efficiency while minimizing the cost of “wiring” the network (Achard and Bullmore, 2007; Bassett and

Bullmore, 2006). Small-world organization allows for network resilience to regional damage. Evaluating pathological brain functioning from this perspective is appropriate in the study of FASD because: 1) only a limited number of network metrics need to be examined; 2) network metrics may be sensitive to developmental changes, allowing for examination of trajectories; 3) the measures may be sensitive to treatment effects; 4) the methods are applicable to younger participants and those with cognitive deficits because no task is needed and shorter MRIs lead to fewer motion artifacts.

The current findings suggest that global measures are useful in understanding the functional consequences of prenatal alcohol exposure. Examining a network of 62 cortical ROIs, we observed correlated brain activity with clear small-world properties. Sigma was equivalent for the two groups, allowing for comparisons of equivalent networks (same cost, number of nodes, and full-connection criteria) (Sporns and Zwi, 2004). Significant differences with moderate effect sizes were seen for *characteristic path length* and *global efficiency*. Children with FASD showed 3% higher characteristic path length than controls and those with FASD had approximately 2% lower global efficiency than controls. Although global efficiency is inversely related to path length, global efficiency is a useful measure because it is more robust when networks are not fully-connected and because it preferentially reflects the contributions of hubs (Achard and Bullmore, 2007). Although we do not yet fully understand the clinical relevance of a 2–3% deficit in network efficiency, this type of network abnormality likely represents a chronic deficit that affects both conscious and unconscious brain functioning 24 hours a day. Because the network properties measured here may reflect capacity for critical “offline” processing, such as planning and memory consolidation (Raichle and Snyder, 2007; Tambini et al., 2010), even a small decrement in efficiency likely has functional consequences. Although correlations were not statistically significant, the data suggest a relationship between immediate memory capacity and both characteristic path length and global efficiency. We did not observe significant correlations between network measures and long-term memory.

Participant age was an important correlate of functional connectivity that we did not examine because of sample size limitations. Prior evidence indicates that functional connectivity changes over early development. In infants, the picture is dominated by strong inter-hemispheric connectivity (Fransson et al., 2011) but there is a shift toward increased cortical-cortical connectivity from childhood to adulthood (Supekar et al., 2009). Little is known about the developmental unfolding of structural and functional brain anomalies in FASD, but their presentation may vary by developmental stage. Longitudinal data will ultimately be necessary to fully understand these functional connectivity abnormalities.

We did not observe group differences in cortical thickness, but network status was correlated with cortical thickness. After partialling out age, one finding remained significant: thinner frontal cortex was associated with lower global efficiency. Others have reported both thicker cortex in FASD compared to controls (Sowell et al., 2008b) and thinner cortex in FASD (Zhou et al., 2011). One potential reason for these discrepancies may be the diagnostic makeup of the groups: In the Sowell study, 67% had dysmorphic facial features whereas only 15% did in the Zhou study. In the current study, 50% had facial dysmorphia. Differences in facial characteristics across samples suggest possible differences in the pattern and timing of alcohol exposure. This, in turn, could have contributed to differences in cortical thickness across samples. Previous studies showed an association between cortical thickness and cognitive functions. Shaw et al. (2006) reported that cortical thickness was negatively correlated with IQ in younger children, but positively associated with IQ in older children and adolescents. It is possible that we did not observe a significant relationship between cortical thickness and IQ because the study included children from ages 10 to 17.

There are limitations to the specificity of our findings. Psychiatric co-morbidity is a reality in FASD (Streissguth and O'Malley, 2000). We included participants with common co-morbidities to maximize generalizability of the results. Children with ADHD (a common co-morbidity in FASD) have functional connectivity abnormalities (Tomasi and Volkow, 2012). Within our FASD sample, we evaluated connectivity in those with and without ADHD and did not observe differences. Medication status was not a significant contributor to network connectivity. Another potential confound is the known association between resting-state connectivity and in-scanner motion (Satterthwaite et al., 2012). Increased motion is associated with either increased or decreased connectivity, depending on the network measure. This potential confound is concerning in children (who move more than adults) and in clinical populations (like FASD) who frequently have hyperactivity. We addressed this at several levels, including the elimination of participants with excessive motion, the use of motion correction, and testing for group differences in motion (there were none).

The conclusions from resting-state studies must be tempered by the novelty of the methods. Although resting-state connectivity measures are reliable (Braun et al., 2012), including in children, the reliability varies somewhat depending on pre-processing and data handling steps (Braun et al., 2012). More broadly, the interpretation of results is partly dependent on pre-processing decisions. For example, the application of global signal regression remains controversial because it introduces negative correlations whose neurophysiological meaning is debated (Fox et al., 2009). Global signal regression introduces anti-correlations but is recommended because it enhances specificity (Weissenbacher et al., 2009). We applied global signal regression based on Weissenbacher's observation that it reduces noise and increases specificity. Resting-state connectivity methods are still in their infancy and interpretive questions remain, yet the methods show great promise in characterizing pathological brain functioning.

Global functional connectivity measures may someday serve as quantitative metrics of brain status in studies of clinical populations. Such metrics could be useful in examining subgroups, further exploring relationships with cognitive functioning, and evaluating the efficacy of new FASD interventions. Certainly, connectivity abnormalities of this kind are not specific to FASD and there are important confounds to examine such as co-morbid ADHD and other psychiatric conditions. Nonetheless, functional connectivity explorations are likely to lead to important advancements in our understanding of the full range of effects of prenatal alcohol exposure.

Acknowledgments

This work was supported by the National Institutes of Health (5P41RR008079, 5K12RR023247, P30-NS057091,& MO1-RR00400), the MIND Institute, and the Minnesota Supercomputing Institute.

References

Achard S, Bullmore E. Efficiency and cost of economical brain functional networks. PLoS Comput Biol. 2007; 3:e17. [PubMed: 17274684]

Archibald SL, Fennema-Notestine C, Gamst A, Riley EP, Mattson SN, Jernigan TL. Brain dysmorphology in individuals with severe prenatal alcohol exposure. Dev Med Child Neurol. 2001; 43:148–54. [PubMed: 11263683]

Astley SJ, Clarren SK. Diagnosing the full spectrum of fetal alcohol-exposed individuals: introducing the 4-digit diagnostic code. Alcohol Alcohol. 2000; 35:400–10. [PubMed: 10906009]

Bassett DS, Bullmore E. Small-world brain networks. Neuroscientist. 2006; 12:512–23. [PubMed: 17079517]

Biswal B, Yetkin FZ, Haughton VM, Hyde JS. Functional connectivity in the motor cortex of resting human brain using echo-planar MRI. Magn Reson Med. 1995; 34:537–41. [PubMed: 8524021]

Bookstein FL, Connor PD, Huggins JE, Barr HM, Pimentel KD, Streissguth AP. Many infants prenatally exposed to high levels of alcohol show one particular anomaly of the corpus callosum. Alcohol Clin Exp Res. 2007; 31:868–79. [PubMed: 17386071]

Braun U, Plichta MM, Esslinger C, Sauer C, Haddad L, Grimm O, Mier D, Mohnke S, Heinz A, Erk S, Walter H, Seiferth N, Kirsch P, Meyer-Lindenberg A. Test-retest reliability of resting-state connectivity network characteristics using fMRI and graph theoretical measures. Neuroimage. 2012; 59:1404–12. [PubMed: 21888983]

Bullmore E, Sporns O. Complex brain networks: graph theoretical analysis of structural and functional systems. Nat Rev Neurosci. 2009; 10:186–98. [PubMed: 19190637]

Cohen J. A power primer. Psychol Bull. 1992; 112:155–9. [PubMed: 19565683]

Cox RW. AFNI: software for analysis and visualization of functional magnetic resonance neuroimages. Comput Biomed Res. 1996; 29:162–73. [PubMed: 8812068]

Dale AM, Fischl B, Sereno MI. Cortical surface-based analysis. I. Segmentation and surface reconstruction. Neuroimage. 1999; 9:179–94. [PubMed: 9931268]

Delis, DC.; Kramer, JH.; Kaplan, E.; Ober, BA. California Verbal Learning Test Manual, Children's Version. The Psychological Corporation; San Antonio: 1994.

Delis, DC.; Kramer, JH.; Kaplan, E.; Ober, BA. California Verbal Learning Test. 2. The Psychological Corporation; San Antonio, TX: 2000. (CVLT-II)

Fair DA, Cohen AL, Dosenbach NU, Church JA, Miezin FM, Barch DM, Raichle ME, Petersen SE, Schlaggar BL. The maturing architecture of the brain's default network. Proc Natl Acad Sci U S A. 2008; 105:4028–32. [PubMed: 18322013]

Fair DA, Cohen AL, Power JD, Dosenbach NU, Church JA, Miezin FM, Schlaggar BL, Petersen SE. Functional brain networks develop from a "local to distributed" organization. PLoS Comput Biol. 2009; 5:e1000381. [PubMed: 19412534]

Fox MD, Zhang D, Snyder AZ, Raichle ME. The global signal and observed anticorrelated resting state brain networks. J Neurophysiol. 2009; 101:3270–83. [PubMed: 19339462]

Fransson P, Aden U, Blennow M, Lagercrantz H. The functional architecture of the infant brain as revealed by resting-state fMRI. Cereb Cortex. 2011; 21:145–54. [PubMed: 20421249]

Friston KJ, Frith CD, Liddle PF, Frackowiak RS. Functional connectivity: the principal-component analysis of large (PET) data sets. J Cereb Blood Flow Metab. 1993; 13:5–14. [PubMed: 8417010]

Fryer SL, Schweinsburg BC, Bjorkquist OA, Frank LR, Mattson SN, Spadoni AD, Riley EP. Characterization of White Matter Microstructure in Fetal Alcohol Spectrum Disorders. Alcohol Clin Exp Res. 2009; 33:1–8. [PubMed: 18828798]

Gioia, GA.; Isquith, PK.; Guy, SC.; Kenworthy, L. Behavior Rating Inventory of Executive Function (BRIEF). Psychological Assessment Resources, Inc; Lutz, FL: 2000.

Greve DN, Fischl B. Accurate and robust brain image alignment using boundary-based registration. Neuroimage. 2009; 48:63–72. [PubMed: 19573611]

Hoyme HE, May PA, Kalberg WO, Kodituwakku P, Gossage JP, Trujillo PM, Buckley DG, Miller JH, Aragon AS, Khaole N, Viljoen DL, Jones KL, Robinson LK. A practical clinical approach to diagnosis of fetal alcohol spectrum disorders: clarification of the 1996 institute of medicine criteria. Pediatrics. 2005; 115:39–47. [PubMed: 15629980]

Latora V, Marchiori M. Efficient behavior of small-world networks. Phys Rev Lett. 2001; 87:198701. [PubMed: 11690461]

Lebel C, Rasmussen C, Wyper K, Walker L, Andrew G, Yager J, Beaulieu C. Brain diffusion abnormalities in children with fetal alcohol spectrum disorder. Alcoholism: Clinical and Experimental Research. 2008; 23:1732–1740.

Li L, Coles CD, Lynch ME, Hu X. Voxelwise and skeleton-based region of interest analysis of fetal alcohol syndrome and fetal alcohol spectrum disorders in young adults. Hum Brain Mapp. 2009; 30:3265–3274. [PubMed: 19278010]

Liu Y, Liang M, Zhou Y, He Y, Hao Y, Song M, Yu C, Liu H, Liu Z, Jiang T. Disrupted small-world networks in schizophrenia. Brain. 2008; 131:945–61. [PubMed: 18299296]

Ma X, Coles CD, Lynch ME, Laconte SM, Zurkiya O, Wang D, Hu X. Evaluation of corpus callosum anisotropy in young adults with fetal alcohol syndrome according to diffusion tensor imaging. Alcohol Clin Exp Res. 2005; 29:1214–22. [PubMed: 16046877]

Raichle ME, MacLeod AM, Snyder AZ, Powers WJ, Gusnard DA, Shulman GL. A default mode of brain function. Proc Natl Acad Sci U S A. 2001; 98:676–82. [PubMed: 11209064]

Raichle ME, Snyder AZ. A default mode of brain function: a brief history of an evolving idea. Neuroimage. 2007; 37:1083–90. discussion 1097-9. [PubMed: 17719799]

Riley EP, Mattson SN, Sowell ER, Jernigan TL, Sobel DF, Jones KL. Abnormalities of the corpus callosum in children prenatally exposed to alcohol. Alcohol Clin Exp Res. 1995; 19:1198–202. [PubMed: 8561290]

Riley EP, McGee CL, Sowell ER. Teratogenic effects of alcohol: a decade of brain imaging. Am J Med Genet C Semin Med Genet. 2004; 127:35–41. [PubMed: 15095470]

Roussotte FF, Rudie JD, Smith L, O'Connor MJ, Bookheimer SY, Narr KL, Sowell ER. Frontostriatal Connectivity in Children during Working Memory and the Effects of Prenatal Methamphetamine, Alcohol, and Polydrug Exposure. Dev Neurosci. 2012; 34:43–57. [PubMed: 22472800]

Rubinov M, Sporns O. Complex network measures of brain connectivity: uses and interpretations. Neuroimage. 2010; 52:1059–69. [PubMed: 19819337]

Santhanam P, Coles CD, Li Z, Li L, Lynch ME, Hu X. Default mode network dysfunction in adults with prenatal alcohol exposure. Psychiatry Res. 2011; 194:354–62. [PubMed: 22079659]

Satterthwaite TD, Wolf DH, Loughead J, Ruparel K, Elliott MA, Hakonarson H, Gur RC, Gur RE. Impact of in-scanner head motion on multiple measures of functional connectivity: relevance for studies of neurodevelopment in youth. Neuroimage. 2012; 60:623–32. [PubMed: 22233733]

Shaw P, Greenstein D, Lerch J, Clasen L, Lenroot R, Gogtay N, Evans A, Rapoport J, Giedd J. Intellectual ability and cortical development in children and adolescents. Nature. 2006; 440:676–9. [PubMed: 16572172]

Smith SM, Jenkinson M, Woolrich MW, Beckmann CF, Behrens TE, Johansen-Berg H, Bannister PR, De Luca M, Drobnjak I, Flitney DE, Niazy RK, Saunders J, Vickers J, Zhang Y, De Stefano N, Brady JM, Matthews PM. Advances in functional and structural MR image analysis and implementation as FSL. Neuroimage. 2004; 23(Suppl 1):S208–19. [PubMed: 15501092]

Sowell ER, Johnson A, Kan E, Lu LH, Van Horn JD, Toga AW, O'Connor MJ, Bookheimer SY. Mapping white matter integrity and neurobehavioral correlates in children with fetal alcohol spectrum disorders. J Neurosci. 2008a; 28:1313–9. [PubMed: 18256251]

Sowell ER, Mattson SN, Kan E, Thompson PM, Riley EP, Toga AW. Abnormal cortical thickness and brain-behavior correlation patterns in individuals with heavy prenatal alcohol exposure. Cereb Cortex. 2008b; 18:136–44. [PubMed: 17443018]

Sporns O, Zwi JD. The small world of the cerebral cortex. Neuroinformatics. 2004; 2:145–62. [PubMed: 15319512]

Spottiswoode BS, Meintjes EM, Anderson AW, Molteno CD, Stanton ME, Dodge NC, Gore JC, Peterson BS, Jacobson JL, Jacobson SW. Diffusion tensor imaging of the cerebellum and eyeblink conditioning in fetal alcohol spectrum disorder. Alcohol Clin Exp Res. 2011; 35:2174–83. [PubMed: 21790667]

Streissguth AP, O'Malley K. Neuropsychiatric implications and long-term consequences of fetal alcohol spectrum disorders. Semin Clin Neuropsychiatry. 2000; 5:177–90. [PubMed: 11291013]

Supekar K, Musen M, Menon V. Development of large-scale functional brain networks in children. PLoS Biol. 2009; 7:e1000157. [PubMed: 19621066]

Tambini A, Ketz N, Davachi L. Enhanced brain correlations during rest are related to memory for recent experiences. Neuron. 2010; 65:280–90. [PubMed: 20152133]

Tomasi D, Volkow ND. Abnormal functional connectivity in children with attention-deficit/hyperactivity disorder. Biol Psychiatry. 2012; 71:443–50. [PubMed: 22153589]

van den Heuvel MP, Stam CJ, Kahn RS, Hulshoff Pol HE. Efficiency of functional brain networks and intellectual performance. J Neurosci. 2009; 29:7619–24. [PubMed: 19515930]

Watts DJ, Strogatz SH. Collective dynamics of 'small-world' networks. Nature. 1998; 393:440–2. [PubMed: 9623998]

Wechsler, D. Wechsler Adult Intelligence Scale. 3. The Psychological Corporation; San Antonio: 1997.

Wechsler, D. Wechsler Intelligence Scale for Children. 4. The Psychological Corporation; San Antonio, TX: 2003.

Weissenbacher A, Kasess C, Gerstl F, Lanzenberger R, Moser E, Windischberger C. Correlations and anticorrelations in resting-state functional connectivity MRI: a quantitative comparison of preprocessing strategies. Neuroimage. 2009; 47:1408–16. [PubMed: 19442749]

Woolrich MW, Jbabdi S, Patenaude B, Chappell M, Makni S, Behrens T, Beckmann C, Jenkinson M, Smith SM. Bayesian analysis of neuroimaging data in FSL. Neuroimage. 2009; 45:S173–86. [PubMed: 19059349]

Wozniak JR, Mueller BA, Chang PN, Muetzel RL, Caros L, Lim KO. Diffusion tensor imaging in children with fetal alcohol spectrum disorders. Alcohol Clin Exp Res. 2006; 30:1799–806. [PubMed: 17010147]

Wozniak JR, Mueller BA, Muetzel RL, Bell CJ, Hoecker HL, Nelson ML, Chang PN, Lim KO. Inter-hemispheric functional connectivity disruption in children with prenatal alcohol exposure. Alcohol Clin Exp Res. 2011; 35:849–61. [PubMed: 21303384]

Wozniak JR, Muetzel RL, Mueller BA, McGee CL, Freerks MA, Ward EE, Nelson ML, Chang PN, Lim KO. Microstructural corpus callosum anomalies in children with prenatal alcohol exposure: an extension of previous diffusion tensor imaging findings. Alcohol Clin Exp Res. 2009; 33:1825–35. [PubMed: 19645729]

Yang Y, Roussotte F, Kan E, Sulik KK, Mattson SN, Riley EP, Jones KL, Adnams CM, May PA, O'Connor MJ, Narr KL, Sowell ER. Abnormal Cortical Thickness Alterations in Fetal Alcohol Spectrum Disorders and Their Relationships with Facial Dysmorphology. Cereb Cortex. 2011

Zhou D, Lebel C, Lepage C, Rasmussen C, Evans A, Wyper K, Pei J, Andrew G, Massey A, Massey D, Beaulieu C. Developmental cortical thinning in fetal alcohol spectrum disorders. Neuroimage. 2011; 58:16–25. [PubMed: 21704711]

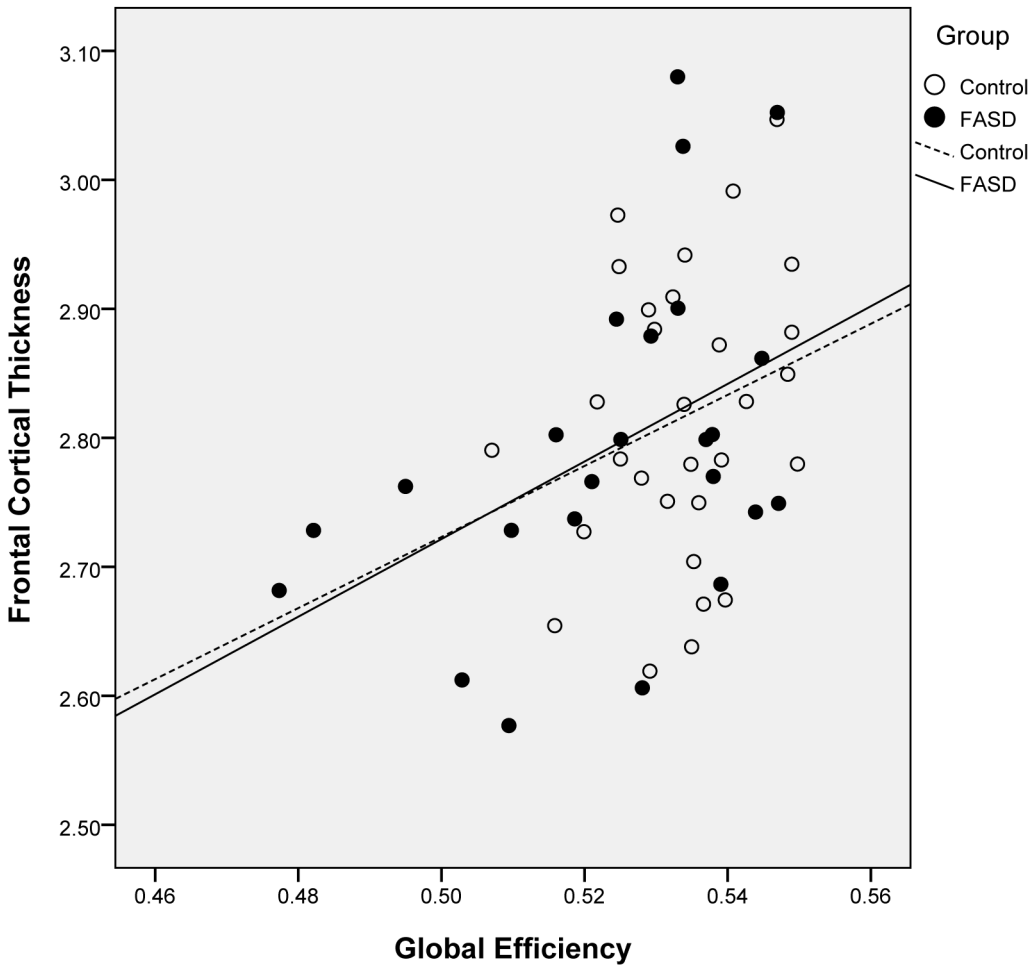

Figure 1.
Illustration of the relationship between cortical thickness in bilateral frontal regions and global efficiency for participants with Fetal Alcohol Spectrum Disorder and control subjects.

Table 1

Demographic characteristics of included participants.

N(%) or mean ± SD	FASD (n=24)	Control (n=31)	Statistical Test
Age at MRI scan	14.3 ± 2.2 yrs.	13.7 ± 2.3 yrs.	t=−.987, p=.77
Gender			
Male	13 (54%)	17 (55%)	
Female	11 (46%)	14 (45%)	χ^2=.002, p=.960
Handedness			
Right	24 (100%)	31(100%)	
Growth			
Height	62.7 ± 4.8 in.	64.1 ± 6.4 in.	t=.884, p=.381
Weight	118 ± 34 lbs.	129 ± 50 lbs.	t=.931, p=.356
Facial Features			
1. None	5 (21%)	-	-
2. Mild	7 (29%)	-	-
3. Moderate	4 (17%)	-	-
4. Severe	8 (33%)	-	-
Alcohol Exposure			
1. No Risk	0 (0%)	-	-
2. Unknown Risk	4 (16%)	-	-
3. Some Risk	15 (63%)	-	-
4. High Risk	5 (21%)	-	-
4-Digit Classification (Astley & Clarren)			
"Other FASD" including Sentinel Physical Findings & Static Encephalopathy	15 (63%)	-	-
Partial FAS	7 (29%)	-	-
FAS	2 (8%)	-	-
Modified IOM Diagnosis (Hoyme)			
FAS without confirmation of alcohol	2 (8%)	-	-
Partial FAS with confirmation of alcohol	9 (38%)	-	-
Partial FAS without confirmation of alcohol	2 (8%)	-	-
ARND	11 (46%)	-	-
Co-morbid-diagnoses			
Attention Deficit Hyperactivity Disorder	15 (63%)	-	-
Oppositional Defiant Disorder	8 (33%)	-	-
Depressive Disorder	4 (17%)	-	-
Anxiety Disorder	3 (13%)	-	-
Reactive Attachment Disorder	3 (13%)	-	-
Learning Disability	2 (8%)	-	-
Medications			
No Medications	10 (42%)	31 (100%)	-
Stimulants	10 (42%)	-	-
SSRIs	5 (21%)	-	-

N(%) or mean ± SD	FASD (n=24)	Control (n=31)	Statistical Test
Atypical antipsychotics	2 (8%)	-	-
Sleep medicine	2 (8%)	-	-
Medicine for tics (guanfacine, clonidine)	2 (8%)	-	-
SNRI	1 (4%)	-	-
Cognitive Functioning			
Verbal Comprehension Index	86 ± 10.9	113 ± 13.2	t=8.20, p<.001
Perceptual Reasoning Index	88 ± 15.8	116 ± 13.3	t=7.25, p<.001
Working Memory Index	85 ± 17.9	108 ± 12.2	t=5.69, p<.001
Processing Speed Index	86 ± 15.8	102 ± 11.9	t=4.31, p<.001
Full-Scale IQ	83 ± 13.5	114 ± 12.0	t=9.20, p<.001
CVLT Total Score	43 ± 11.5	57 ± 7.6	t=5.69, p<.001
CVLT Trial 1	−.23 ± 1.1	.52 ± .83	t=2.90, p=.005
CVLT Long Delay Free Recall	−.75 ± 1.0	.48 ± .70	t=5.38, p<.001
BRIEF General Executive Composite	71 ± 16.3	44 ± 7.4	t=−8.05, p<.001

NOTE: ARND = Alcohol Related Neurobehavioral Disorder; SSRI = Selective Serotonin Re-uptake Inhibitor; SNRI = Selective Norepinephrine Re-uptake Inhibitor; CVLT = California Verbal Learning Test (children's version [CVLT-C] or adult version [CVLT-2]);

Table 2

MRI sequence and parameters.

Sequence	Imaging Parameters	Purpose	Time
T1-weighted MPRAGE	TR=2350 ms, TE=3.65 ms, TI=1100 ms, 224 slices, voxel size= 1×1×1 mm, FOV=256 mm, flip angle=7 degrees, GRAPPA 2.	Segmentation & cortical parcellation	5 min
Resting fMRI	TR=2000 ms, TE=30 ms, 34 interleaved slices, no skip, voxel size= 3.45×3.45×4.0 mm, FOV=220 mm, flip angle=77 degrees, 180 measures.	Measurement of BOLD signal	6 min
fMRI field map	Positioned to match fMRI: TR=700 ms, TE=1.91 ms & 3.37 ms, 34 slices, voxel size=3.45×3.45×4.0 mm, FOV=220 mm, flip angle=90 degrees.	Correction for geometric distortions of fMRI	1 min

Table 3

Group differences in network properties for FASD and control groups at cost = 0.20.

Mean ± SD	FASD (n = 24)	Control (n = 31)	% Difference	Cohen's d Effect size
Characteristic Path Length	2.27 ± 0.19	2.20 ± 0.09	3.1%	0.47**
Mean Clustering Coefficient	0.58 ± 0.05	0.56 ± 0.04	3.5%	0.44*
Local Efficiency	0.76 ± 0.03	0.75 ± 0.03	1.3%	0.33*
Global Efficiency	0.52 ± 0.02	0.53 ± 0.01	1.9%	0.63**

* trend level of p<.1;

** significant at p<.05;

Table 4

Correlations between network connectivity measures and regional cortical thickness measures (FASD and control groups combined).

	Characteristic Path Length (CPL)	CPL (partial correlation with age)	Global Efficiency (GE)	GE (partial correlation with age)
Frontal lobe cortical thickness	r=−.36, p=.008 *	r=−.26, p=.057	r=.38, p=.005 **	r=.28, p=.044 *
Temporal lobe cortical thickness	r=−.25, p=.066	r=−.15, p=.172	r=.28, p=.043 *	r=.17, p=.218
Parietal lobe cortical thickness	r=−.35, p=.009 *	r=−.26, p=.064	r=.36, p=.008 *	r=.25, p=.075
Occipital lobe thickness	r=−.18, p=.198	r=−.08, p=.559	r=.19, p=.168	r=.09, p=.530

NOTE:

* significant correlation p<.05;

** significant correlation after correction for multiple comparisons.

Table 5

Correlations between network connectivity measures and cognitive performance (FASD group only).

	Characteristic Path Length	Global Efficiency
Wechsler VCI	r=.18, p=.41	r=−.19, p=.38
Wechsler POI	r=.23, p=.28	r=−.23, p=.28
Wechsler WMI	r=.18, p=.39	r=−.15, p=.48
Wechsler PSI	r=.23, p=.29	r=−.27, p=.21
CVLT Total Score	r=−.18, p=.41	r=.21, p=.32
CVLT Trial 1 (immediate memory)	r=−.41, p=.05 *	r=.41, p=.01 **
CVLT Long Delay Free Recall (delayed memory)	r=−.11, p=.63	r=.16, p=.47
BRIEF General Executive Composite	r=.41, p=.05 *	r=.13, p=.54

NOTE:

* trend level correlation;

** significant correlation p<.05;

VCI = Verbal Comprehension Index; POI = Perceptual Organization Index;

WMI = Working Memory index; PSI = Processing Speed Index; CVLT = California Verbal Learning Test (children's version [CVLT-C] or adult version [CVLT-2])